Journal of Simulation & Analysis of Novel Technologies in Mechanical Engineering
12(4) (2019) 0067~0080
HTTP://JSME.IAUKHSH.AC.IR
ISSN: 2008-4927

# Investigating the Effect of Solid Solution Treatment on the Corrosion Properties of Biodegradable Mg-Zn-RE-xCa (x = 0, 2.5) Alloy

Saeed Alibabaei[1], Masoud Kasiri-Asgarani[1]*, Hamid Reza Bakhsheshi-Rad[1]

1. *Advanced Materials Research Center, Department of Materials Engineering, Najafabad Branch, Islamic Azad University, Najafabad, Iran. **

Manuscript Received --- 14 Ap. 2020; Revised --- 28 Jun. 2020; Accepted --- 15 Jul. 2020)

**Abstract**

In this study, the effect of heat treatment on the corrosion properties of Mg-Zn-RE-xCa alloy (x = 0, 2.5) was investigated. These alloys were produced using an argon atmosphere casting process and then subjected to vacuum conditions at 400 C for 6 hours under solid solution treatment and quenching in water. The microstructure and fuzzy analysis of heat treatment alloys using optical microscope (OM), X-ray diffraction (XRD), scanning electron microscope (SEM) and energy-dispersive X-ray spectroscopy (EDS) were investigated. Immersion, polarization, impedance, and pH changes test were performed to study alloy corrosion behavior. The results showed that in heat treated samples, the values of secondary phases IM1 (Ca3MgxZn15-x) ($4.6 \leq x \leq 12$) and Mg2Ca increased with increasing calcium content. However, the amount of these phases is reduced by dissolution and quenching in water. The corrosion density of alloy is reduced by adding 2.5% calcium from 488.4 to 315 μA / $cm^2$, which decreases to 126.5 μA / $cm^2$ after 6 hours of heat treatment, indicating improved corrosion resistance of the alloy after heat treatment.

*Keywords:* Magnesium - Solution Thermal Operations - Biodegradability - Polarization

## *1. Introduction*

Substances of natural and artificial origin that are used to improve, treat, heal or replace tissue in living organisms are called biomaterials. Biomaterials are divided into four types: metal, polymer, ceramic and composite, among which metallic biomaterials have been used more due to their high strength, toughness, flexibility and availability. Metallic biomaterials must be non-degradable and biodegradable in this context include stainless steels, titanium and its alloys, cobalt-chromium alloys, magnesium alloys, etc.

Biomaterials must have appropriate physical, corrosion, mechanical and biological properties. On the other hand, the formability and being cost-effective and availability are very important factors for selecting biomaterials [1]. In this regard, the first biodegradable and absorbable implants were polymers, including polyglycolic acid, polylactic acid, and polydioxanone [2-4]. However, the use of polymeric materials for load-bearing applications is severely limited due to their low strength [5]. Recently, magnesium and its alloys have received much attention due to their similar mechanical properties to bone, including the density of 31.74 g / $cm^3$ and the 45 gigapascal Yang modulus, which causes a sharp reduction in the stress shielding phenomenon [6, 7]. Magnesium density is 1.6 and 4.5 times lower than that of aluminum and steel, respectively. Magnesium and its alloys, as biodegradable

implants, do not require secondary surgery to be removed from the body compared to traditional implants such as stainless steel, titanium alloys, etc. [6, 8, 9]. Moreover, according to the literature, an adult consumes between 300 and 400 mg of magnesium daily, so too much magnesium is not harmful to the body and is excreted from the urine [11, 12]. However, poor corrosion resistance of magnesium, which leads to rapid loss of mechanical strength in the physiological environment of the body, has limited its use. The two main reasons for its corrosion are as follows. On the one hand, magnesium alloys are very active metals and their thin surface oxide layer cannot protect from the substrate well, and on the other hand, having suitable composition and uniform structures has great effect on the occurrence of galvanic corrosion of magnesium. Therefore, the microstructure of magnesium alloy plays an important role in its corrosion mechanism. So, the effects of microstructure and composite in the corrosion behavior of magnesium alloys have been extensively investigated [1].

Alloying and heat treatment are among the solutions to increase the corrosion resistance of magnesium alloys [13]. Heat treatment can alter the microstructure and distribution of metal elements, which has a significant effect on the corrosion behavior of the alloy. One of the most important magnesium alloys used in biomaterials are Mg-Zn and Mg-Ca systems.

In this connection, Zinc is one of the essential elements of the body and can strengthen the mechanical strength and rapid formation of Mg-Zn sediments through precipitation hardening, which increases the strength and corrosion resistance of magnesium-based alloys.

In this view, Calcium is also a major component of bone, and adding a small amount of calcium to the Mg-Zn alloy improves mechanical properties, and the release of calcium particles can improve bonding and bone formation. In addition, to some extent, due to the formation of stable intermetallic compounds, it causes the grain to become fine and strengthens the grain boundary [13, 14].

It is worth noting that, other common elements used for alloying and adding to magnesium base alloys include aluminum, manganese, copper, yttrium, zirconium, and rare earth elements that improve the physical and mechanical properties of magnesium alloys. Alloying elements must be carefully selected to maintain the biocompatibility of magnesium and not cause toxicity [15].

Among the magnesium based alloys, magnesium-zinc-calcium alloy has also attracted special attention in research and industry. In recent years, this alloy has been considered as a new candidate for biodegradable implants for biomedical applications. These interests in magnesium-zinc-calcium alloys are due to the beneficial role of zinc and calcium in improving mechanical properties as well as their lower cost compared to other alloying elements in magnesium-based systems [16]. Studies on Mg – 0.5Ca – xZn alloys (x = 0–9 wt%) have shown that the atomic ratio of calcium/zinc determines that $Mg_2Ca$ or $Ca_2Mg_6Zn_3$ or both are formed in the microstructure. $Mg_2Ca$ and $Ca_2Mg_6Zn_3$ are two important intermetallic compounds that are formed in three-component alloys of Mg-Zn-Ca, and depending on the chemical composition of the alloy, one or both of them can be formed during the freezing process. The presence of these two intermetallic phases makes alloy hardening [17]. It has been well established that the addition rare elements (RE) such as cerium is an effective way to improve the mechanical properties of magnesium alloys in high temperature. Growing of the stable phase of $Mg_{12}Ce$ has been observed at the grain boundary during creep and this phase seems to reduce the amount of deformation caused by the grain boundary slip. In addition, rare earth elements generally have a positive effect on corrosion resistance of magnesium

alloys. Rare earth (RE) metals are elements of the seventeenth group with similar properties, but when they are added to the magnesium, there is a significant difference between them. Highly popular Misch metals that are added to magnesium include a combination of cerium with lanthanum, neodymium. In Mg-Ce alloys rich magnesium, two phases were consistent with the formulas $Mg_{12}Ce$ and $Mg_{17}Ce$. Alloying elements of RE used to solve magnesium problems are mainly rare elements with high solubility in magnesium. The designed alloys are close to a single-phase solid solution. Recent results have shown that the addition of rare earth elements is a very promising way to improve the ductility and corrosion of magnesium alloys. In addition, the addition of rare earth elements in magnesium alloys increases the stability of the passive film on the surface, which will be useful for improving corrosion resistance. Improving corrosion resistance for Mg-RE alloys may be related to the following: Firstly, adding rare earth elements can purify the magnesium matrix during casting and remove some harmful elements such as iron. Secondly, the stability of the passive film can be improved by adding rare earth elements. Thirdly, solid single-phase solution without impurity will be very useful for reducing galvanic corrosion [18, 19].

Thus, the aim of this study was to investigate the simultaneous effect of RE elements with Zn and Ca alloying elements (variable) as well as the effect of solution heat treatment and alloy element on the mechanical, corrosion and biological properties of magnesium based alloy.

## 2. *Materials and Method*

Granules and ingots of Mg-32Ca and Mg-2.2Zn-3.7RE were used to prepare the alloy studied in this study, respectively. RE elements in this alloy ingot included wt 70% cerium, wt 25% lanthanum and wt 5% neodymium.

To obtain magnesium alloys with different amounts of calcium (0 and 2.5 wt%), measurements were made according to Equations 2-1 and 2-2.

$$\text{Calcium weight} = \frac{(\text{Mg}-2.2\text{Zn}-3.7\text{RE Alloy weight}) \times \text{Calcium wt\%}}{\text{Mg}-2.2\text{Zn}-3.7\text{RE Alloy wt\%}} \quad (1\text{-}2)$$

$$\text{Mg}-32\text{Ca Alloy weight} = \frac{100 \times \text{Calcium weight}}{32} \quad (2\text{-}2)$$

The weighted materials were melted in a high-frequency induction furnace using a steel mold under argon shielding gas to reduce the reaction of magnesium with air. The melting temperature was maintained for 30 minutes at 760ºC to ensure complete and uniform melting of the alloys. After the melting and alloying processes, the molten metal was combined with various amounts of calcium (0 and 2.5%) in a preheated mold at 400ºC to produce ingots.

Subsequently, Heat treatment was performed at 400ºC for 6 hours in an ATRA vacuum furnace.

In order to observe the microstructure of the samples and compare them in terms of the amount or distribution of the eutectic phase, the samples were first polished with 800-4000 sandpapers and being snitched free surface. They were then polished by POLISEC-C25 polishing machine manufactured by PRESI at a speed of 450 rpm for 1 min with $Al_2O_3$ solution.

The microstructural characteristics were determined by Optical Microscope (OM), X-ray diffraction (XRD), Fourier Transform-Infrared Spectroscopy (FTIR), Scanning Electron Microscope (SEM) and Energy-dispersive X-ray spectroscopy (EDS).

Electrochemical, pH variations, and immersion test in simulated body fluid (SBF) were performed to investigate the corrosion behavior of the sample.

A standard three-electrode cell was used to test the potentiodynamic polarization. The saturated calomel electrode (SCE) and graphite electrodes were used as reference electrodes and auxiliary electrodes, respectively. The test was performed on Ringer's solution at 37ºC. The PARSTAT2273 device was used to perform the test. The samples were placed in a special cell containing 50 ml of Ringer's solution. The impedance spectrum was measured at a frequency of 1 Hz to 100 kHz, and the samples were analyzed using Zview software. In order to ensure the accuracy of the results, 3 measurements were performed for each sample and polarization and impedance curves were obtained.

The immersion and pH variations tests were performed according to NACE TM0169/G31-12a standard at 37ºC. The samples were immersed in a Ringer solution with the pH=7.4 and placed in an incubator. Due to the high corrosion rate of magnesium alloys, a 24-hour time interval was selected to measure the pH, and the pH was measured every 24 hours. The immersed samples were washed with distilled water and dried at room temperature. X-ray diffraction (XRD and Fourier Transform-Infrared Spectroscopy (FTIR) were used to analyze corrosion products. Scanning electron microscope was also used to assess the surface properties of the samples eaten.

## *3. Results and Discussion*

### *3.1. Microstructural characterization*

Figure (1) shows the microstructure of Mg-Zn-RE-xCa alloys (x = 0, 2.5%) before and after heat treatment. The microstructure of all alloys includes α–Mg matrix and eutectic phases.

Figure (A-B -1) shows the microstructure of the alloys before heat treatment. As can be seen, by adding 2.5% calcium to the alloy, dark phases appear in the microstructure. The microstructure of the alloy containing 2.5% calcium indicates a smaller grain size, which indicates the effect of calcium on retinning the grain size. This phenomenon can be attributed to the formation of secondary phase and eutectic compounds. Witte & et al. [20] reported that calcium acts as a factor in reducing grain size and is known as the borderline reinforcing phase.

Figure (C-D -1) shows the microstructure of heat treatment alloys at a temperature of 400ºC and a time interval of 6 hours. As can be seen, similar to the microstructure of alloys before heat treatment, it remains almost unchanged and includes α-mg matrix and eutectic phases, which the dark spots on the microstructure also increase by adding 2.5% calcium. After 6 hours of heat treatment, very little tendency to dissolve eutectic compounds and grain growth is observed, which can be justified according to the fuzzy diagram (Figure 2) [21]. According to the diagram, after dissolving at 400ºC for Mg-Zn-RE alloy, the presence of magnesium HCP structure and $Mg_{12}RE$, IM1[1] and $CeMgZn_2$ phases is confirmed. As calcium levels increase, in addition to the presence of magnesium HCP structure and $Mg_{12}RE$ and IM1 phases, $Mg_2Ca$ phase is also observed. However, as shown in Figure (D-1), some of the eutectic phases are dissolved and a more uniform structure is observed than before the heat treatment. Zhang et al. [22] also reported that the microstructure of Mg-Zn-Ca alloys containing rare earth elements remains almost unchanged after heat treatment of the solution, and the dissolution of eutectic compounds is very limited. On the other hand, the presence of cerium and lanthanum elements in Mg-Zn-Ca alloy due to the presence of $Mg_{12}RE$ phase leads to improved thermal stability of the alloy [23].

The microstructure and distribution of the secondary phase of Mg-Zn-RE-xCa (x = 0, 2.5) alloys can be clearly seen before the heat treatment with SEM images (Figure 3).

[1] $(Ca_3Mg_xZn_{15-x})$ $(4.6 \leq x \leq 12)$

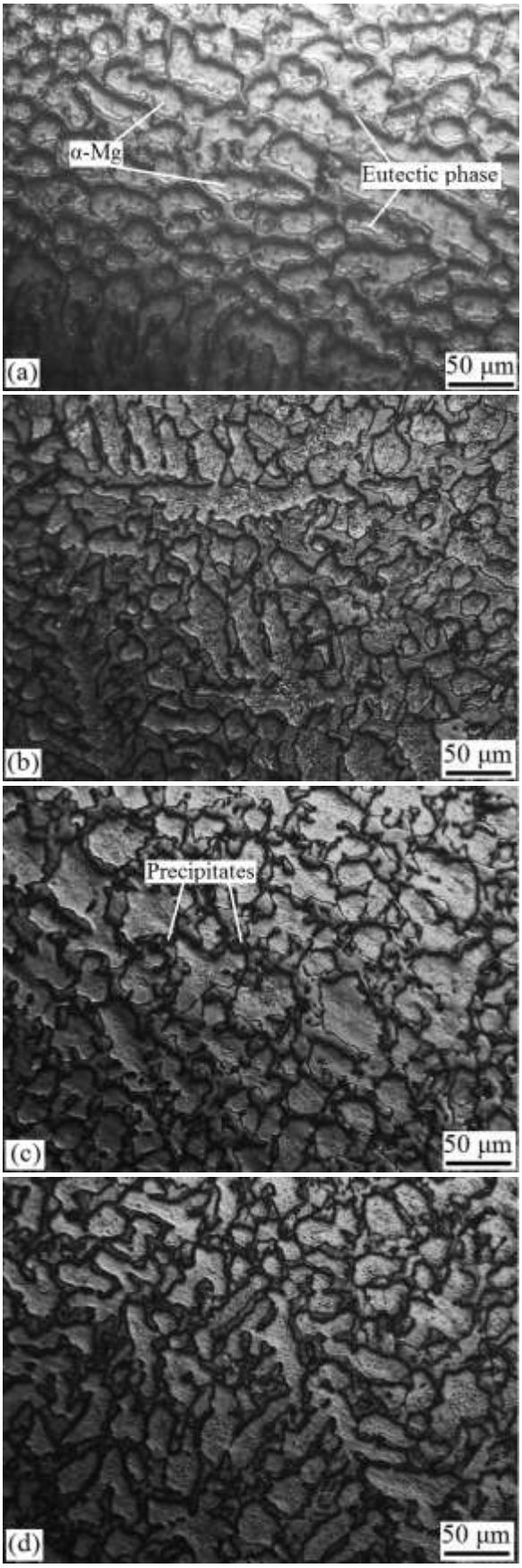


Figure 1: Mg-Zn-RE-xCa (x = 0, 2.5) alloy microstructure before heat treatment; (A) 0% calcium, (b) 2.5% calcium, after heat treatment; (C) 0% calcium, (d) 2.5% calcium

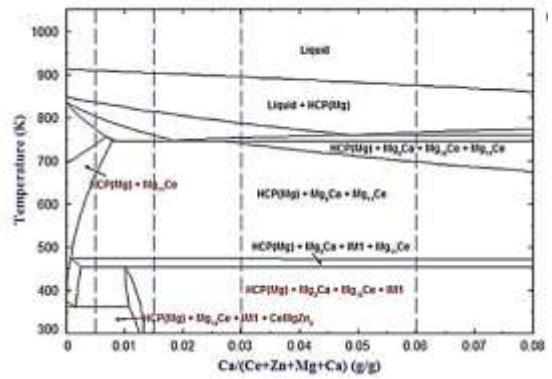


Figure 2: phase diagram of Mg-Zn-RE-xCa quaternary system [21]

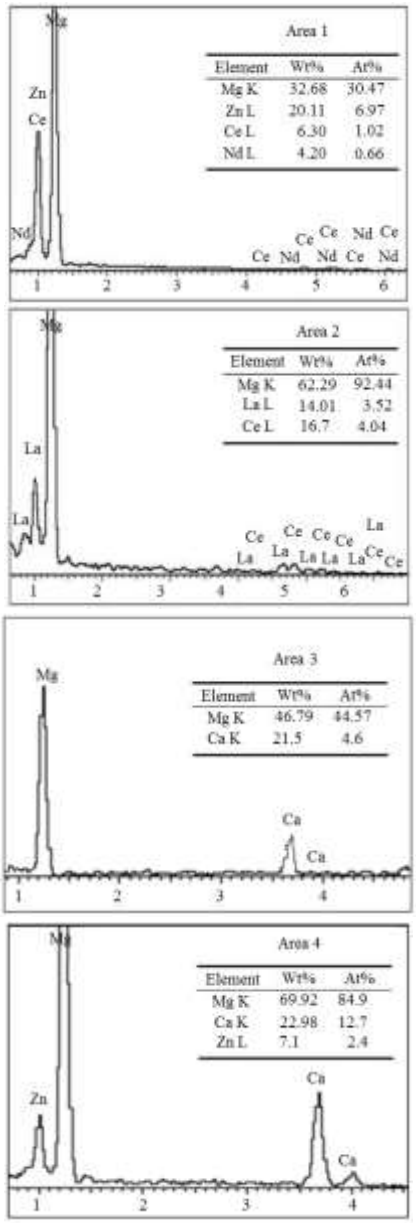


Figure 3: Mg-Zn-RE-xCa (x = 0, 2.5) alloy SEM images before heat treatment; (A) 0% calcium, (c) 2.5% calcium, EDS; (B) Zone 1, (d) Zone 2, (e) Zone 3 and (f) Zone 4

Figure (3-a) includes two dark and light areas, the bright areas are related to $Mg_{12}RE$ phase and the dark areas are related to α-Mg phase. In addition, there is some $CeMgZn_2$ phase in the α-Mg matrix, which can be verified by fuzzy diagram (Figure 1) and EDS analysis (Figure 3, area 1-2). Adding calcium to the alloy leads to the formation of intermetallic phases. The IM1 and $Mg_{12}RE$ phases are stable compounds that are present alongside magnesium. When 2.5% calcium is added to the alloy, a layered structure is observed. Figure (3b) shows the presence of $Mg_2Ca$, $Mg_{12}RE$ and α-Mg layered phases, and EDS analysis (Figure 3, area 4-5) also confirms the presence of these phases. Research by Levy et al. [24] shows that the Mg-1.6Ca-3.2Zn microstructure consists of a separate α-Mg matrix which is separated by the $Mg_2Ca$ and $Ca_2Mg_6Zn_3$ eutectic phases.

Figure (4) shows the microstructure and distribution of the secondary phase of Mg-Zn-RE-xCa (x = 0, 2.5) alloys after heat treatment. According to the results of optical microscope images, SEM images also show that eutectic phases have not been completely dissolved, but the coherence and uniformity of these phases were not absent. In Figure (4-a), similar to cast alloy, the microstructure of heat-treated alloys also includes two dark and light areas, the dark area is related to α-Mg phase and the light area is related to $Mg_{12}RE$ phase. Moreover, the $CeMgZn_2$ phase, which was present in the cast alloy, was dissolved in large quantities in the magnesium matrix of the heat-treated alloy. The intermetallic phases of $Mg_2Ca$ and IM1 formed by the addition of calcium to the alloy have been greatly reduced after the heat treatment of the solution compared to the cast alloys, and the resulting layered structures have been reduced. As shown in Figure (4-b), the dissolution of eutectic phases and their uniformity reduction in alloys containing 2.5% calcium is more than in alloys without calcium. It was also obvious that some parts of the eutectic phases have also disappeared.

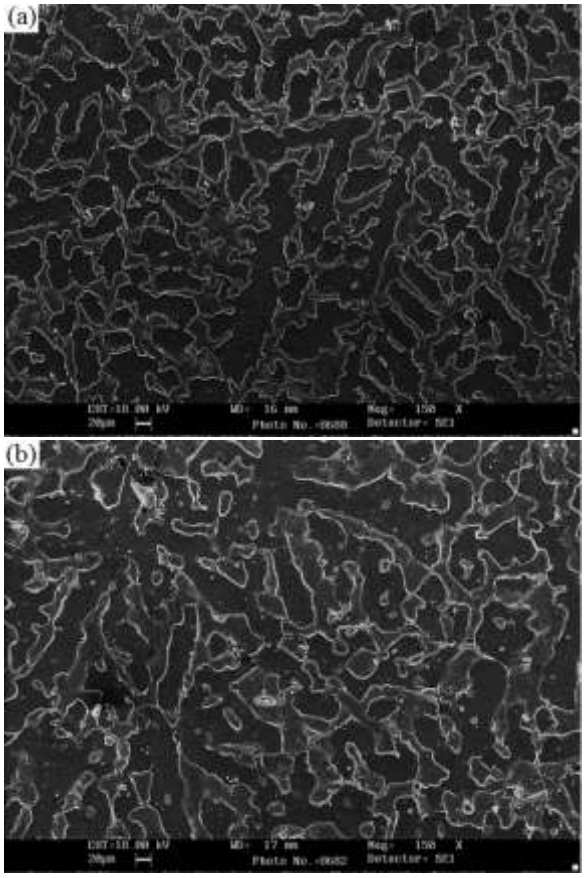

Figure 4: Mg-Zn-RE-xCa (x = 0, 2.5) alloy SEM images after heat treatment; (A) 0% calcium, (c) 2.5% calcium

### *3.2. Phase analysis*

Figure (5) shows the X-ray diffraction analysis of Mg-Zn-RE-xCa alloy (x = 0, 2.5) before and after heat treatment. Figure (a) shows the XRD pattern of the Mg-Zn-RE alloy before heat treatment, in which there is an intensity of peaks of the α-Mg and $Mg_{12}RE$ phases. According to the XRD patterns, the Mg-Zn-RE-xCa alloy has the highest peak intensity available for all samples in the α-Mg and $Mg_{12}RE$ phases, and is eliminated by adding calcium to the $CeMgZn_2$ phase alloy. By adding 2.5% calcium to the alloy before heat treatment, the peaks of the $Mg_2Ca$ phase appear (Figure 3-4 b). In addition to the α-Mg, $Mg_2Ca$ and $Mg_{12}RE$ peaks, there are other additional peaks for this alloy, some of which are related to the IM1 interphase phase. IM1 consists of ($Ca_3Mg_xZn_{15-x}$) ($4.6 \leq x \leq 12$) at 335ºC with hexagonal structure. John et al. [25] reported that

the $Mg_2Ca$ phase can be easily observed in calcium-containing alloys.

Figure (5 c-d) is the analysis of XRD after heat treatment, which is very little different from the casting sample. According to the results of XRD alloys before heat treatment, the intensity of peaks of diffusion of phase's α-Mega and $Mg_{12}RE$ is quite evident for the sample without calcium (Figure 5-c). For samples containing 2.5% calcium after heat treatment (Figure 5-d), a decrease in peak intensity of $Mg_2Ca$ and IM1 peaks and sometimes an increase in peak intensity of α-mg and $Mg_{12}RE$ phases is observed. According to previous results, heat treatment has not completely eliminated the $Mg_2Ca$ and IM1 phases, but has reduced their intensity peak.

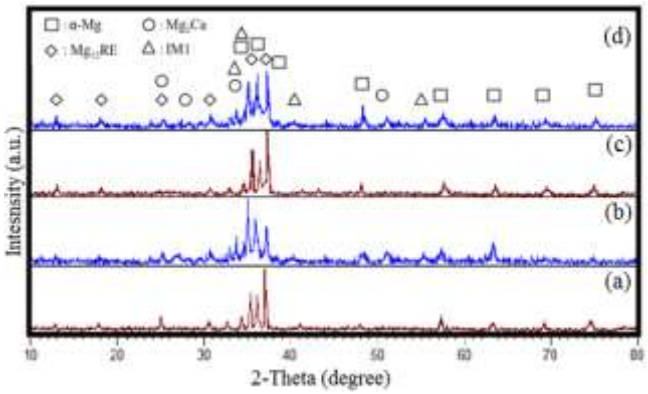


Figure 5: X-ray diffraction analysis of Mg-Zn-RE-xCa (x = 0, 2.5) alloy before heat treatment; (a) 0% calcium, (b) 2.5% calcium, after heat treatment; (c) 0% calcium, (d) 2.5% calcium

### *3.3. Corrosion behavior of Mg-Zn-RE-xCa*

Electrochemical corrosion tests were performed using polarization and impedance tests in Ringer's solution to evaluate and compare the biodegradability behavior of Mg-Zn-RE-xCa (x = 0, 2.5 wt%) alloy before and after heat treatment.

The results show that the corrosion potential ($E_{corr}$) of Mg-Zn-RE alloy is about -1841 mVSCE, which has the highest negative value compared to alloys containing calcium. This phenomenon shows that the cathode reaction in quaternary alloys is more difficult than in ternary alloys. By adding 2.5% calcium, the corrosion potential changes to -1775 mVSCE, which is more positive than the Mg-Zn-RE alloy.

As can be seen, heat treatment has a significant effect on the polarization curve and increases the corrosion potential, which indicates the improvement of corrosion properties of alloys after heat treatment. The results show that after heat treatment, the highest negative value of corrosion potential is related to the Mg-Zn-RE ternary alloy (-1573 mVSCE) and confirms that the cathodic reaction in quaternary alloys is more difficult than in ternary alloys. The results after the heat treatment are in accordance with the results of the alloys before the heat treatment and the best corrosion potential is related to the calcium-containing sample after the heat treatment. Table 3-1 shows the corrosion potential ($E_{corr}$) and the corrosion current *density* ($i_{corr}$) of the samples before and after the heat treatment. As can be seen, the highest corrosion potential belongs to the sample containing 2.5% calcium after heat treatment.

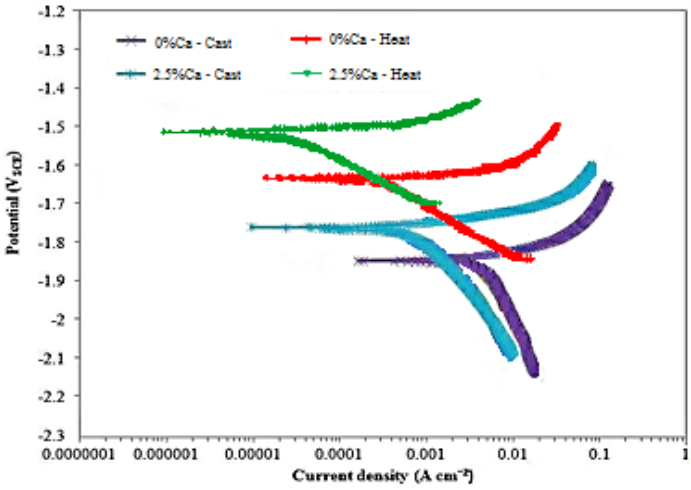


Figure 6: The polarization curve of the Mg-Zn-RE-xCa (x = 0, 2.5) alloy before and after heat treatment

Figure (7) shows the surface morphology and EDS analysis of Mg-Zn-RE-xCa (x = 0, 2.5) alloy before heat treatment after 168 hours of immersion in the Ringer solution. Figure (7-a) shows large cracks and cavities in the inner layer and precipitate in the outer part. When 2.5%

calcium is added to the ternary alloy, the original geometric shape is preserved and fewer cracks are present on the surface (Figure 7-b). Parts of the surface were also covered with white particles of brucite $Mg(OH)_2$ solution, which were identified by EDS analysis. These corrosion products act as a protective layer to protect the surface against corrosive solutions and increase corrosion resistance [26].

Table 1: Electrochemical parameters of Mg-Zn-RE-xCa (x = 0, 2.5) alloy before and after heat treatment

| | sample | Corrosion potential $E_{corr}$(mV) | Corrosion current density $i_{corr}$($\mu A/cm^2$) | Corrosion rate (mmpy) |
|---|---|---|---|---|
| Before heat treatment | Mg-Zn-RE | -1841 | 488.4 | 8.17 |
| | Mg-Zn-RE-2.5Ca | -1755 | 316 | 5.28 |
| After heat treatment | Mg-Zn-RE | -1573 | 194.8 | 3.25 |
| | Mg-Zn-RE-2.5Ca | -1532,6 | 127 | 2.12 |

The white particles are in the form of needle shape apatite similar to the human bone collagen matrix (Figure 7-c). Surface needle-shaped morphology, which has had more contact with SBF solution, causes more apatite to form on the surface for bone repair [27]. EDS analysis of needle morphology also indicates the formation of HA with the presence of magnesium, phosphorus, oxygen and carbon. Due to the richness of the surface of RE, it was difficult to detect calcium (Figure 7-d). The presence of oxygen in the protective layer is due to hydrocarbons and $Mg(OH)_2$. The presence of carbon can also be attributed to the hydrocarbons obtained from the environment [28].

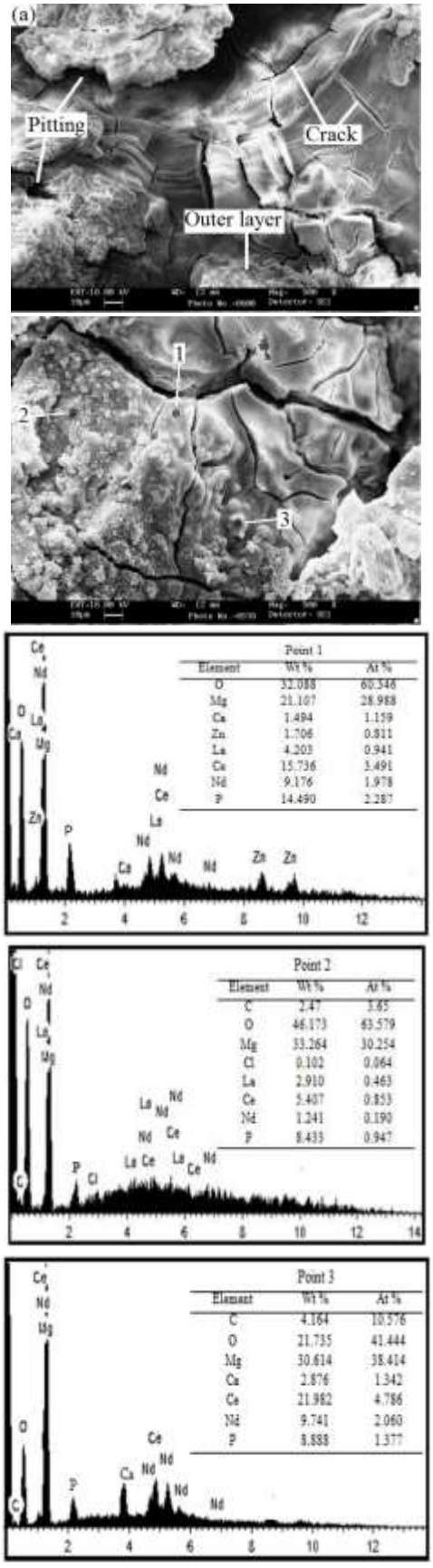


Figure 7: The SEM images of Mg-Zn-RE-xCa (x = 0, 2.5) alloy before heat treatment and after 168 hours of immersion; (a) 0% calcium, (b) 2.5% calcium, (c) area X, EDX

EDS analysis (Figure 7-c) of the corrosion layer showed that the corrosion product was composed of magnesium, oxygen, rare earth elements (cerium, lanthanum, neodymium), as well as some phosphorus, zinc, and calcium. The atomic ratio of oxygen to magnesium (O/Mg) is 2.22, which indicates the formation of $Mg(OH)_2$. However, the outer layer is composed of carbon, oxygen, magnesium, calcium, and phosphorus, indicating the presence of hydroxyapatite (Fig 7-e).

Figure (8) shows the surface morphology and EDS analysis of Mg-Zn-RE-xCa (x = 0, 2.5) alloy after heat treatment after 168 hours of immersion in the SBF. As can be seen, after the heat treatment of the solution, the amount and size of cracks and cavities decreased. According to the results of the polarization test (Figure 8), the highest corrosion is related to the Mg-Zn-RE ternary alloy. By adding 2.5% calcium, the corrosion resistance increases, and comparison of it with the sample that did not has thermal operations shows that after the heat treatment, the corrosion resistance has increased significantly. On the other hand, the amount corrosion product containing HA formed on the surface of heat-treated alloys is higher than the alloys before heat treatment.

Figure (9) shows the XRD pattern of Mg-Zn-RE-xCa (x = 0, 2.5 wt%) alloy corrosion products before and after heat treatment, after 168 hours of immersion in Ringer solution. The XRD pattern represents the presence of $Mg(OH)_2$ along with Mg and HA. As you can see, adding calcium to the alloy also increases the intensity of the $Mg(OH)_2$ peak.

As can be seen after the heat treatment, the corrosion products are similar to the samples before the heat treatment, but the difference is in the amounts of these products. Heat treatment has led to a reduction in the intensity of $Mg(OH)_2$ peaks, resulting in improved corrosion resistance. Peaks related to HA have not changed significantly, and as a result, heat treatment has not significantly improved the biological properties.

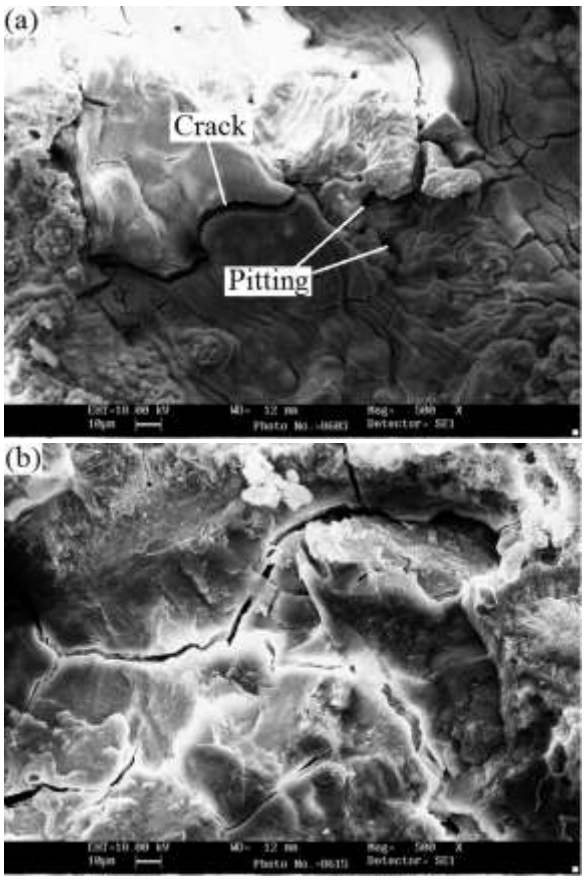


Figure 8: The SEM images of Mg-Zn-RE-xCa (x = 0, 2.5 wt%) alloy after heat treatment and 168 hours of immersion; (a) 0% calcium, (b) 2.5% calcium

The specific peak in the range of 2θ in the range of 20-80 degrees indicates the formation of hydroxyapatite [28]. It was also observed that the addition of calcium leads to further formation of HA phases, which indicates the formation of more corrosion products on the surface of the sample. $Mg(OH)_2$ porosity, which is formed in the early stages of the corrosion process, acts as a protective layer for the deposition of calcium and phosphorus. However, the presence of Cl-ions in Ringer solution contributes to the degradation of $Mg(OH)_2$, resulting in more cavities on the surface [29].

FTIR spectra of Mg-Zn-RE-xCa (x = 0, 2.5) alloy products before and after heat treatment, after 168 hours of immersion in SBF solution are shown in

Figure 10. Obviously, the corrosion products formed on the surface of the alloys before and after the heat treatment are similar, but their values are different. The strong and sharp peak at 3704 $cm^{-1}$, is related to O-H traction which confirms that the formation of $Mg(OH)_2$ has a corrosion product layer [30].

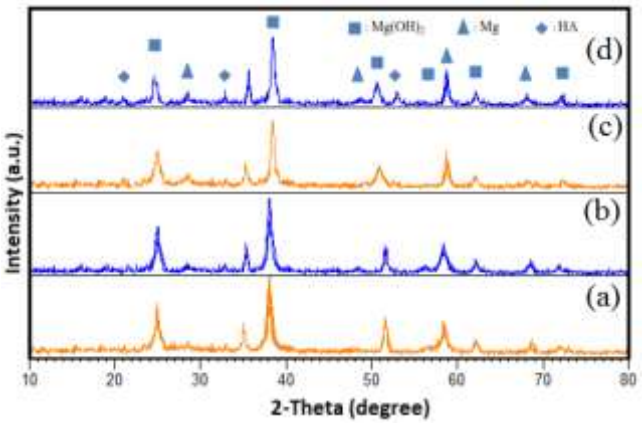


Figure 9: XRD analysis of Mg-Zn-RE-xCa (x = 0, 2.5) alloy after 168 hours of immersion; before heat treatment; (A) 0% calcium, (b) 2.5% calcium, after heat treatment; (C) 0% calcium, (d) 2.5% calcium

The large adsorption band from 3664 to 3215 $cm^{-1}$ and also the adsorption in 3448 $cm^{-1}$ are attributed to the vibration of water molecules. The phosphate group ($PO_4^{-3}$) was determined as about 1047 to 1170 $cm^{-1}$ for V3 mode and 560 $cm^{-1}$ for V2 mode. This type of phosphate is more similar to biological apatite and can be a good alternative to bone [31]. Weak bands in 2934 $cm^{-1}$ can also be attributed to phosphate groups.

A band in 889 $cm^{-1}$ is dedicated to the V2 vibration mode of carbonate groups that are compatible with the spectrum of apatite compounds. The results of FTIR and XRD after immersion indicate the formation of large amounts of corrosion products consisting of magnesium hydroxide and hydroxyapatite on the alloy surface.

Heat treatment reduces the peak intensity of $Mg(OH)_2$, which is consistent with the results of XRD. It can also be observed that the absorption of $Mg(OH)_2$ spectra in the Mg-Zn-RE-2.5Ca heat-treated alloy is lower, which leads to less cracks than other alloys (Figure 8). Decrease in $Mg(OH)_2$ peak indicates an improvement in corrosion resistance that is consistent with other results.

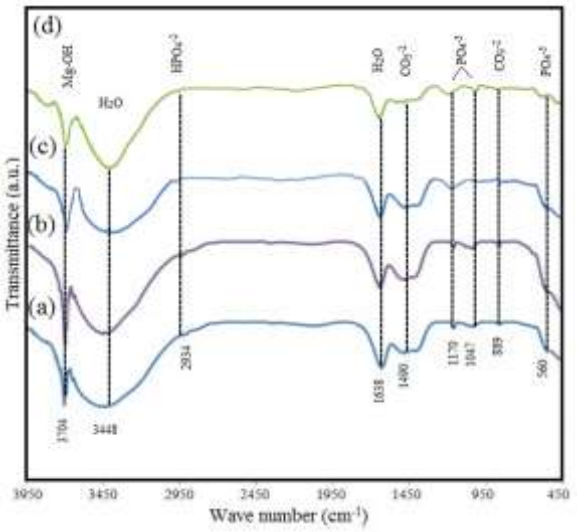


Figure 10: The FTIR of Mg-Zn-RE-xCa (x = 0, 2.5) alloy after 168 hours of immersion; before heat treatment; (A) 0% calcium, (b) 2.5% calcium, after heat treatment; (C) 0% calcium, (d) 2.5% calcium

Figure 11 shows the difference in pH values of Mg-Zn-RE-xCa (x = 0, 2.5) alloy before and after heat treatment after 168 hours of immersion in Ringer solution. Zhang and Young (2009) stated that increasing the pH leads to hemolysis by about 66%, which is not suitable for cell growth and proliferation. Therefore, the pH values of the solutions should be controlled during the immersion test.

The results show that the pH of the solution for all samples in the first stage of immersion increased significantly with increasing duration. The initial increase in pH is due to the accumulation of OH- ions in the form of $Mg(OH)_2$ at the surface of the samples [17]. High pH levels and the presence of $HCO^{3-}$, $HPO_4^{2-}$, $Mg^{2+}$ and $Ca^{2+}$ can lead to increased HA deposition on the surface of Mg-Zn-RE-xCa alloys [32].

However, as the immersion time increases, the pH values stabilize. The highest pH is for calcium-free alloys. By adding 2.5% calcium, the pH of

the Mg-Zn-RE alloy decreases. The high corrosion rate of Mg-Zn-RE alloy, which is related to its high pH, is also confirmed by the polarization curve (Figure 6). High pH accelerates the deposition of magnesium phosphate and carbonate and also stabilizes magnesium hydroxide [33].

The heat treatment of the alloy reduced the pH of the samples during immersion. Similar to heat treated alloys, the rate of increase in pH in the first stage of immersion is high and decreases with increasing time. The results of electrochemical and immersion tests showed that Mg-Zn-RE-2.5Ca alloy has the highest corrosion resistance after heat treatment of the solution, which is also consistent with the pH test results.

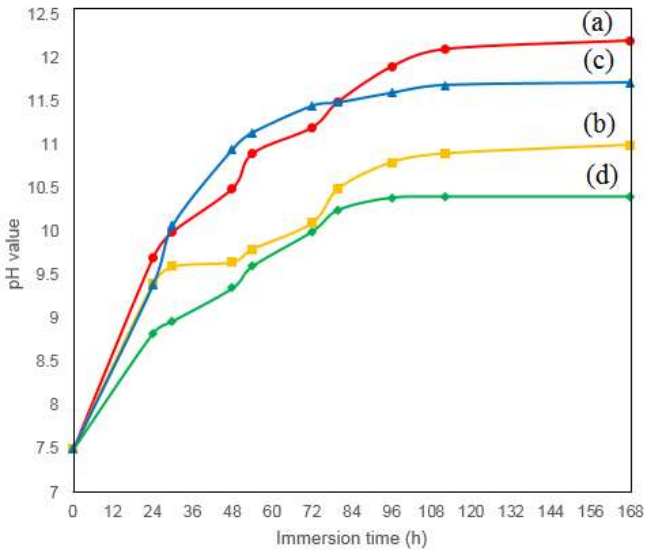


Figure 11: Mg-Zn-RE-xCa alloy pH change chart (x = 0, 2.5) after 168 hours of immersion; Before heat treatment; (A) 0% calcium, (b) 2.5% calcium, after heat treatment; (C) 0% calcium, (d) 2.5% calcium

## *4. Conclusion*

The aim of this study was to improve the corrosion and degradability properties of Mg-Zn-RE-xCa (x = 0, 2.5) alloy by heat treatment. Based on the results of the experiments, it can be concluded that:

1- By adding calcium to Mg-Zn-RE alloy, due to the formation of secondary phases, grain size and α-mg field are reduced, which heat treatment leads to increase in grain size.

2- The microstructure of Mg-Zn-RE-xCa (x = 0, 2.5) alloy before heat treatment includes α-Mg, $Mg_{12}RE$ eutectic and $Mg_{29}Zn_{25}RE$ phase formation, which by adding 2.5% calcium to the Mg-Zn-RE alloy, a structure is composed of IM1 (Ca3MgxZn15-x) phases ($4.6 \leq x \leq 12$) and $Mg_2Ca$. Moreover, the microstructure of the alloys after heat treatment includes α-Mg and Mg12RE phases in low amount and the formation of $Mg_{29}Zn_{25}RE$ disappeared in the structure after calcium addition.

3- The formation of secondary phases has a significant effect on the corrosion rate of Mg-Zn-RE-xCa (x = 0, 2.5) alloy. Adding 2.5% calcium increased corrosion resistance. Heat treatment led to a slight decrease in the secondary phases, followed by an increase in the corrosion resistance of the alloy.

## *References*

[1] Zheng ,Y,F . Gu ,X,N .Witte ,F "Biodegradable metals" ,Materials Science and Engineering, 77 , 1–34 , 2014.

[2] Narayanan T,S,N,S . Park ,S . Lee ,M,H. "Strategies to improve the corrosion resistance of microarc oxidation (MAO) coated magnesium alloys for degradable implants: prospects and challenges" , Materials Science, 60 , 1–71 , 2014.

[3] Montemor ,M,F. "Functional and smart coatings for corrosion protection: a review" ,Surface and Coatings Technology , 258 , 17–37, 2014.

[4] Hornberger ,H . Virtanen ,S . Boccaccini ,A,R "Biomedical coatings on magnesium alloys – a review". Acta Biomaterialia ;8:2442–2455, 2012.

[5] Paital ,S,R . Dahotre ,N,B "Calcium phosphate coatings for bio-implant applications: materials, performance factors, and methodologies" Materials Science and Engineering, 66, 1–70, 2009.

[6] Wu ,G . Ibrahim ,J,M . Chu ,P,K "Surface design of biodegradable magnesium alloys – a review" Surface and Coatings Technology , 233, 2–12, 2013.

[7] Zhang ,H,X. Wang ,Z,N . Zhou ,Y,G. et al. "Temperature evolution analysis of AZ31B

magnesiumalloy during quasistatic fracture" Mater Sci Technol ,32 ,1276–1281 ,2016.

[8] Chen ,Y . Xu ,Z . Smith,C . et al "Recent advances on the development of magnesium alloys for biodegradable implants". Acta Biomaterialia , 10, 4561–4573 , 2014.

[9] Zhou ,L . Liu ,Y . Zhang ,J . et al. "Microstructure and mechanical properties of equal channel angular pressed Mg–Y–RE–Zr alloy". Materials Science Technology.;32:969–975 .2016.

[10] Gu ,X . Zheng ,Y . Cheng ,Y . "In vitro corrosion and biocompatibility of binary magnesium alloys". Biomaterials. ,30 ,484–498, 2009.

[11] Sanchez ,A,H,M . Luthringer ,B,J,C . Feyerabend ,F . et al. "Mg and Mg alloys: how comparable are in vitro and in vivo corrosion rates: A review". Acta Biomaterialia. 13, 16–31, 2015.

[12] Witte ,F . "The history of biodegradable magnesium implants: a review". Acta Biomaterialia., 6, 1680–1692, 2010.

[13] Bakhsheshi-Rad ,H,R . Idris ,M,H . Kadir ,M,R,A . et al. "Microstructure analysis and corrosion behavior of biodegradable Mg–Ca implant alloys". Materials and Design. 33, 88–97, 2012.

[14] Zheng ,Y,F . Gu ,X,N . Xi ,Y,L . et al. "In vitro degradation and cytotoxicity of Mg/Ca composites produced by powder metallurgy". Acta Biomaterialia.;6:1783–791. 2010.

[15] Bakhsheshi-Rad ,H,R . Hamzah ,E . Low ,H,T . et al. "Fabrication of biodegradable Zn-Al-Mg alloy: mechanical properties, corrosion behavior, cytotoxicity and antibacterial activities". Materials Science and Engineering C.;73: 215–219, 2017.

[16] Wu,G . Ibrahim, J.M . Chu,P.K . "Surface design of biodegradable magnesium alloys _ A review"; Surface and Coatings Technology, 233, 2-12, 2013.

[17] Bakhsheshi-Rad, H.R., Abdul-Kadir, M.R., Idris, M.H., Farahany, S., "Relationship between the corrosion behavior and the thermal characteristics and microstructure of Mg-0.5Ca-xZn alloys". Corrosion Science, 64:184–97, 2012.

[18] Bakhsheshi-Rad, H., Abdellahi, M., Hamzah, E., Bahmanpour, M., "Modelling corrosion rate of biodegradable magnesium-based alloys:The case study of Mg-Zn-RE-xCa (x ¼ 0, 0.5, 1.5, 3 and 6 wt%) alloys"; Journal of Alloys and Compounds, 687, 630-642, 2016.

[19] Zhou, W.R., Zheng ,Y.F., Leeflang ,M.A., Zhou, J., "Mechanical property, biocorrosion and in vitro biocompatibility evaluations of Mg-Li-(Al)-(RE) alloys for future cardiovascular stent application". Acta Biomaterialia. 9 (10):8488–98. 2013.

[20] Witte ,F . Hort ,F. Vogt ,N . Cohen ,C . Kainer ,S . "Degradable Biomaterials Based on Magnesium Corrosion". Current Opinion in Solid State and Materials Science, 12, 63-72, 2008.

[21] Bakhsheshi-Rad. H.R , Hamzah, E . Joy , S,L . Medraj. M , Idris. M. H , Mostafa ,A ; "Characterisation and thermodynamic calculations of biodegradable Mg–2.2Zn–3.7Ce and Mg–Ca–2.2Zn–3.7Ce alloys"; Materials Science and Thechnology, 33, 1333-1345 ,2017.

[22] Zhang ,S,X . Zhang ,X,N . Zhao ,C,L . et al. "Research on an Mg-Zn alloy as a degrad-able biomaterial". Acta Biomaterialia, 6 (2):626–40, 2010.

[23] Zhou, T. Chen, D. Chen, Z.H. Chen, J.H. "Investigation on microstructures and properties of rapidly solidified Mg–6wt.%Zn–5 wt.% Ca–3 wt.% Ce alloy"; Journal of Alloys and Compounds , 475, L1-L4, 2009.

[24] Levi, G. Avraham, S. Zilberov, A. Bamberger, M.; "Solidification, solution treatment and age hardening of a Mg–1.6 wt.% Ca–3.2 wt.% Zn alloy"; Acta Materialia, 54, 523-530, 2006.

[25] Jun, J. H., Park, B. K., Kim, J. M., Kim, K. T. and Jung, W. J. "Microstructure and Tensile Creep Behavior of Mg-Nd-RE-Ca Casting Alloys". Key Engineering Materials, 345-346, 557-560, 2007.

[26] Cai, S. H . Lei, L . Li ,N,F and Feng ,F. "Effects of Zn on microstructure, mechanical properties and corrosion behavior of Mg-Zn alloys". Materials Science and Engineering C-Materials for Biological Applications, 32 (8):2570–2577, 2012.

[27] Meng, E.C., Guan, S.K., Wang, H.X. and Wang, L.G. "Effect of Electrodeposition Modes on Surface Characteristics and Corrosion Properties of Fluorine-doped Hydroxyapatite Coatings on Mg-Zn-Ca alloy". Applied Surface Science, 257, 4811-4816, 2011.

[28] Li, Z., Gu, X., Lou, S., and Zheng, Y., "The development of binary Mg–Ca alloys for use as biodegradable materials within bone". Biomaterials, 29 (10):1329–44, 2008.

[29] Wang, B., Gao, J.H., Wang, L.G., Zhu, S.J., and Guan, K ., "Biocorrosion of coated Mg-Zn-Ca alloy under constant compressive stress close to that of human tibia". Materials Letters 70:174–6, 2012.

[30] Du, H., Wei, Z.J., Liu, X.W., and Zhang, E.L., "Effects of Zn on the microstructure, mechanical property and bio-corrosion property of Mg-3Ca alloys for biomedical application". Materials Chemistry and Physics, 125 (3):568–75, 2011.

[31] Fahamin, A, Tabrizi, B. and Ebrahimi-Kahrizsangi, R . "Synthesis of Calciumphosphate-based Composite Nanopowders by Mechanochemical Process and Subsequent Thermal Treatment". Ceramics International. 38, 6729-6738, 2012.

[32] Zhang, E., Yin, D., Xu, L., Lei, Y. and Yang, K . "Microstructure, Mechanical and Corrosion Properties and Biocompatibility of Mg–Zn–Mn Alloys for Biomedical Application". Materials Science and Engineering C, 29, 987-993, 2009.

[33] Song, G. L. and Song, S. Z. "A Possible Biodegradable Magnesium Implant Material". Advanced Engineering Materials, 94, 298-302, 2007.